

Long-term Study of Changes in the Orbital Periods of 18 Eclipsing SW Sextantis Stars

David Boyd

West Challow Observatory, OX12 9TX, UK; davidboyd@orion.me.uk

Received April 8, 2023; revised May 18, 2023; accepted May 19, 2023

Abstract SW Sex stars are an informal sub-class of eclipsing nova-like cataclysmic variables. We report 934 new eclipse times measured over the past 17 years for HS 0728+6738 (V482 Cam), SW Sex, DW UMa, HS 0129+2933 (TT Tri), V1315 Aql, PX And, HS 0455+8315, HS 0220+0603, BP Lyn, BH Lyn, LX Ser, UU Aqr, V1776 Cyg, RW Tri, 1RXS J064434.5+334451, AC Cnc, V363 Aur, and BT Mon. When combined with published eclipse times going back in some cases many decades, we show that these binary systems exhibit a range of behaviors, including increasing, decreasing, and possibly oscillating orbital periods. Nevertheless, the duration of these observations is still not long enough to be able to make reliable quantitative statements about their long term behaviors. In addition to these long term trends, we also observed rapid and unusual decreases in the orbital periods of SW Sex and RW Tri during 2017 and 2018, respectively.

1. The SW Sex phenomenon

Nova-like variables are a sub-category of cataclysmic variables (CVs) in which the transfer of hydrogen-rich material from the main sequence secondary star to the white dwarf primary via Roche lobe overflow is sustained at a high rate. This maintains the accretion disc around the primary in a bright state and inhibits the disc instability mechanism responsible for dwarf nova outbursts. The majority of nova-like variables have binary orbital periods longer than 3 hours, which places them above the period gap and in the regime where magnetic braking progressively shrinks the binary orbit and drives mass transfer. Further information on CVs can be found in Patterson (1984), Warner (1995), and Hellier (2001).

The name SW Sex stars was first introduced in Thorstensen *et al.* (1991) to characterise a range of observational properties shared by a number of eclipsing nova-like variables which displayed complex and unusual spectral variation with orbital phase. Prototypes of this informal sub-class were SW Sex, DW UMa, PX And, and V1315 Aql. Honeycutt *et al.* (1986) first noticed that SW Sex (known at the time as PG 1012-029) showed deep eclipses in its continuum but hardly at all in its emission lines, suggesting the presence of a bipolar wind emanating from the accretion disk. Several more so-called SW Sex stars were first identified as variables in the Hamburg Quasar Survey (Hagen *et al.* 1995). The observational characteristics of SW Sex stars are described in Hoard *et al.* (2003). Although initially quite narrow, the definition of SW Sex stars now encompasses most nova-like CVs above the period gap with high mass transfer rates. For a review of our knowledge of the SW Sex phenomenon see Schmidtbreick (2015) and references therein.

SW Sex stars with high orbital inclinations experience deep eclipses which provide a means to measure and monitor their orbital periods. Two motivations for this study, which began in 2006, were to produce accurate eclipse ephemerides for predicting future eclipse times and to investigate if any of the stars deviated from the linear ephemeris expected for a constant orbital period. Several of these stars had not been observed systematically for many years and by combining published data

on eclipse times going back in some cases over many decades with new eclipse measurements, their ephemerides could be updated and the stability of their orbital periods investigated.

We chose 18 SW Sex stars which are deeply eclipsing, observable from the UK, and bright enough to yield accurate eclipse times with amateur-sized telescopes. These are listed in Table 1 with their mean orbital periods and the time span of available observations including new results reported here. All have orbital periods above the period gap. One member of the group, BT Mon, experienced a nova outburst in 1939 and a nova shell has since been observed (Duerbeck 1987). Nova shells have also been imaged around V1315 Aql (Sahman *et al.* 2015) and AC Cnc (Shara *et al.* 2012), evidence of nova eruptions several hundred years ago. AC Cnc and BT Mon have two of the longest orbital periods in the group.

An initial report covering the period 2006 to 2012 was published in the *Journal of the AAVSO* (Boyd 2012), hereafter referred to as Paper 1. Here we report on a continuation of this study to 2023 and present results which now cover a 17-year period.

2. Measuring new eclipse times

Predicted times of primary eclipses were obtained from the ephemerides in Paper 1 and a time-series of images of the field of each star obtained starting well before and ending well after these predicted eclipse times to allow for possible variation in orbital period. All images were made unfiltered to maximize photon statistics with either a 0.25-m or 0.35-m Schmidt-Cassegrain Telescope (SCT) and an SXV-H9 (later SXVR-H9) CCD camera located at West Challow Observatory near Oxford, UK. Image scales with these telescopes were 1.45 and 1.21 arcsec/pixel, respectively. Images were dark subtracted and flat fielded and a magnitude for the star was measured in each image using differential aperture photometry with respect to an ensemble of between three and five nearby comparison stars. Comparison star V band magnitudes with errors were obtained from AAVSO charts or from catalogues available at the start of the study. The same comparison star magnitudes and analysis procedures have been used for each star throughout

the study to maintain consistency. A list of comparison stars used for each variable is given in Table 2. If we were starting the project today, we would choose comparison stars from the AAVSO Photometric All-Sky Survey (Henden *et al.* 2018). The photometry error for each star was calculated using the CCD Equation (Howell 2006). For each comparison star this error was then added in quadrature with the comparison chart magnitude error and a weighted mean magnitude zero point and error was computed for the image. This was then used to compute the magnitude and error of the variable star for that image.

A quadratic polynomial was fitted to the lower section of each eclipse in order to find the time of minimum which was expressed as a Heliocentric Julian Date (HJD). An associated analytical error in the time of minimum was derived from uncertainties in the magnitude measurements. The section of the eclipse used for the polynomial fit was normally between the points of maximum slope of the eclipse ingress and egress. Figure 1 shows examples of eclipse profiles. Uncertainties in individual magnitude measurements are generally smaller than the plotted mark. Some eclipses have rounded minima, some are V-shaped, while others exhibit random fluctuations in light output throughout the eclipse, indicating that the source of these fluctuations has not been eclipsed. Irregular eclipse profiles are more difficult to measure and this can lead to larger uncertainties in measured times of minimum. In what follows we will refer to these uncertainties as errors.

It was generally found that analytical errors from the quadratic fits underestimated the real uncertainty in eclipse times. The scatter in eclipse times for each star over a short interval during which the eclipse times were likely to have varied linearly was examined and the analytical errors scaled to make them consistent with the observed scatter about the linear trend. For stars with the smoothest eclipses, a scaling factor of 3 gave errors consistent with the scatter of eclipse times, while for eclipses with the largest fluctuations a factor of 7 was required. This scaling factor was generally found to be consistent for each star throughout the study.

A total of 898 new eclipse times for the 18 stars in this study have been observed and measured by the author. The number of new eclipse times for each star are listed in Table 1. Based on the ephemerides in Paper 1, cycle numbers were assigned to each new eclipse. Measured eclipse times with errors and corresponding cycle numbers for each of the 18 stars are listed in Tables 3.1 to 3.18. For completeness we also include here the eclipse times given in Paper 1. A further 36 eclipse times for LX Ser were measured by the author from observations of LX Ser by Cook and Dvorak in the AAVSO International Database (Kafka 2021). These are listed in Table 4.

3. Published eclipse times

Altogether 1338 eclipse times for these 18 stars were found in more than 40 published papers and in many issues of *Information Bulletin on Variable Stars* (IBVS), *Bulletin of the Variable Star Observers League in Japan* (BVSOLJ), and *Open European Journal on Variable Stars* (OEJV). The numbers of published eclipse times for each star are listed in Table 1 and

the sources of published eclipse times are given in Table 5. We have not included these already published times here for reasons of space. All times of minimum were expressed in HJD for consistency, including some times originally reported in Barycentric Julian Date (BJD). In several cases errors for these eclipse times were not specified in the literature or the errors given were clearly unrealistically small given the observed spread in eclipse times. In these cases we needed to make a realistic estimate of the error in these eclipse times so they could be included in our analysis with appropriate weights. Each such data set was considered separately and the root-mean-square (rms) residual of all the times in that set calculated with respect to a locally fitted linear ephemeris. This value was then assigned as an error to all the eclipse times in that set.

We found that eclipse times derived from photographic plates generally had a large scatter compared to electronically measured times and in practice did not provide a constraint on fitting an ephemeris, so we decided not to include these in this analysis. Eclipse times for RW Tri in Smak (1995) appeared very discrepant with other times reported around the same period and therefore have not been included in this analysis.

4. O–C analysis

Each observed eclipse time of minimum was given a weight equal to the inverse square of its assigned error. A weighted linear fit of all available eclipse times vs cycle numbers was calculated for each star. This linear ephemeris was used to produce a calculated time for each eclipse. The linear term in the ephemeris is the mean binary orbital period of the star over the time interval spanned by the observations. Observed minus calculated (O–C) times for each eclipse were then plotted vs cycle number to produce an O–C diagram for each star.

An apparently linear trend in an O–C diagram is consistent with a constant orbital period, while O–C trajectories curving upward indicate the orbital period is increasing and curving downward that the orbital period is decreasing. In most cases we also calculated a weighted quadratic fit to the O–C values. This quadratic ephemeris gave a mean rate of change of orbital period. In some cases, there was a suggestion of sinusoidal variation relative to a linear ephemeris or quadratic ephemeris. In these cases, a weighted sinusoidal fit was calculated with respect to the linear or quadratic ephemeris.

Table 6 gives weighted linear ephemerides for each star computed as described above. SW Sex experienced a large change in its behavior in 2017 and two linear ephemerides are given for before and after this change. Table 7 gives weighted quadratic ephemerides and mean rates of period change for stars where these were calculated.

Our effort to make the weights used in these fits more realistic will inevitably have introduced an element of subjectivity. Therefore we do not compute a quantitative goodness of fit metric such as a reduced chi-squared for each fit as this would not be an objective basis for evaluating fit quality. This is particularly true in the case of a nonlinear model where there are recognized problems in interpreting such a metric (Andrae *et al.* 2010).

Table 1. Eclipsing SW Sex stars in this study.

<i>Star name</i>	<i>P_{orb}</i> <i>(hours)</i>	<i>Time span of</i> <i>obs. (years)</i>	<i>New eclipse times</i> <i>measured in this study</i>	<i>Previously published</i> <i>eclipse times</i>
HS 0728+6738 = V482 Cam	3.21	20	44	13
SW Sex = PG 1012-029	3.24	43	49	131
DW UMa = PG1030+590	3.28	39	58	596
HS 0129+2933 = TT Tri	3.35	20	42	30
V1315 Aql	3.35	38	51	80
PX And = PG0027+260	3.51	31	45	44
HS 0455+8315	3.57	21	44	9
HS 0220+0603	3.58	20	37	13
BP Lyn = PG0859+415	3.67	32	45	16
BH Lyn = PG0818+513	3.74	31	43	33
LX Ser = Stepanyan's Star	3.80	42	82 *	74
UU Aqr	3.93	37	53	53
V1776 Cyg = Lanning 90	3.95	35	58	11
RW Tri	5.57	65	58	151
1RXS J064434.5+334451	6.47	18	70	36
AC Cnc	7.21	41	49	19
V363 Aur = Lanning 10	7.71	42	62	19
BT Mon	8.01	45	44	10
Total		616	934	1338

Note: * Includes 36 eclipse times for LX Ser measured by the author from observations of LX Ser by Cook and Dvorak in the AAVSO International Database.

Table 2. Comparison stars used to measure the time of minimum for each star.

<i>Star Name</i>	<i>Comparison Stars Used</i>
HS 0728+6738 = V482 Cam	GSC 4360 0033, GSC 4124 0603
SW Sex = PG 1012-029	GSC 4907 1166, GSC 4907 0207, 2MASS J10145841-0305432
DW UMa = PG1030+590	GSC 3822 0070, GSC 3822 0983, GSC 3822 1157
HS 0129+2933 = TT Tri	GSC 1755 0855, GSC 1755 0871, GSC 1755 0942, GSC 1755 0926, GSC 1755 0982
V1315 Aql	GSC 1049 1329, GSC 1049 1288, GSC 1049 0464
PX And = PG0027+260	GSC 1734 0906, GSC 1734 1620, GSC 1734 0752
HS 0455+8315	GSC 4617 1102, GSC 4617 0542, 2MASS J05071087+8318101, 2MASS J05084059+8316305, 2MASS J 05041189+8321282
HS 0220+0603	GSC 0045 1418, GSC 0045 0338, GSC 0045 1226, GSC 0045 1400, GSC 0045 0626
BP Lyn = PG0859+415	GSC 2986 1255, GSC 2986 1258, GSC 2986 1413, GSC 2986 1427
BH Lyn = PG0818+513	GSC 3421 1055, GSC 3421 0865, GSC 3421 1015
LX Ser = Stepanyan's Star	GSC 1497 1576, GSC 1497 0962, GSC 1497 1643, [HH95] LX Ser-4, [HH95] LX Ser-8
UU Aqr	TYC 5227 0328, GSC 5227 0662, GSC 5227 0399, GSC 5227 0982
V1776 Cyg = Lanning 90	GSC 3572 1508, 2MASS J20234934+4629294, 2MASS J20234988+4632359, 2MASS J20231931+4629502, 2MASS J20233377+4634165
RW Tri	GSC 1774 0082, GSC 1178 0469, GSC 1774 0357, GSC 1774 0002
1RXS J064434.5+334451	[SGH2007] J0644-R, [SGH2007] J0644-S, [SGH2007] J0644-E, [SGH2007] J0644-G, [SGH2007] J0644-M
AC Cnc	GSC 0816 1525, GSC 0816 1021, GSC 0816 1547, GSC 0816 0998, GSC 0816 0862
V363 Aur = Lanning 10	[HH95] V363 Aur-04, [HH95] V363 Aur-19, [HH95] V363 Aur-03
BT Mon	GSC 4803 0262, 2MASS J06433904-0204189, 2MASS J06435331-0202124, 2MASS J06433839-0203003

Note: [HH95] = Henden and Honeycutt (1995), [SGH2007] = Sing et al. (2007)

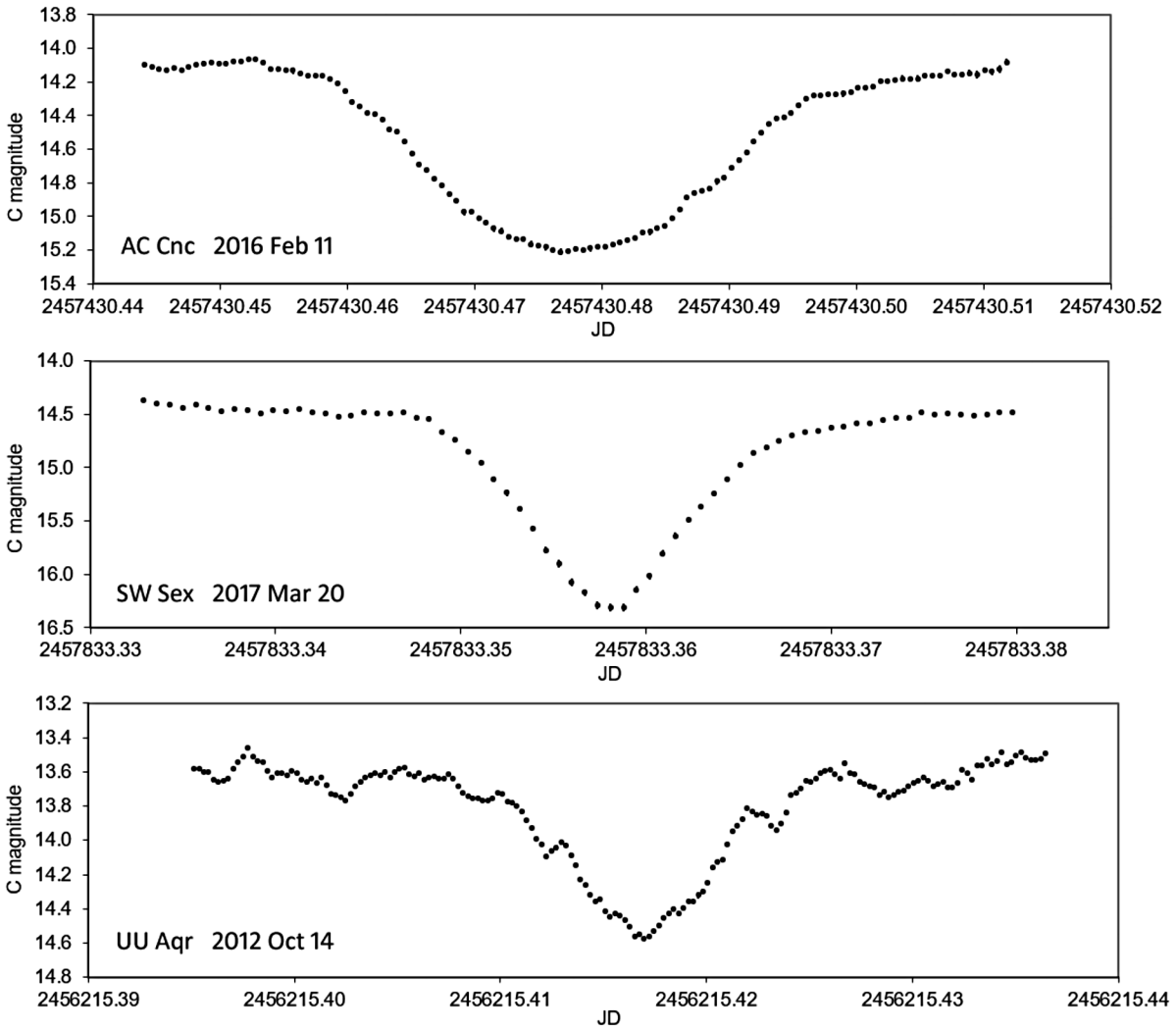


Figure 1. Examples of eclipse profiles. Uncertainties in individual magnitude measurements are generally smaller than the plotted mark.

Table 3.1. Eclipse times, errors and cycle numbers for HS 0728+6738 observed and measured by the author in this study.

<i>Eclipse time (HJD)</i>	<i>Error (d)</i>	<i>Cycle Number</i>
2453810.40077	0.00041	13539
2453836.45653	0.00024	13734
2453851.42254	0.00023	13846
2453853.42648	0.00013	13861
2454174.51418	0.00022	16264
2454181.32859	0.00025	16315
2454185.33706	0.00025	16345
2454186.40643	0.00024	16353
2454473.42029	0.00023	18501
2454493.33001	0.00023	18650
2454507.35967	0.00039	18755
2454835.39541	0.00032	21210
2454891.38182	0.00010	21629
2454895.39084	0.00009	21659
2454907.41644	0.00022	21749
2455188.41832	0.00021	23852
2455191.35834	0.00014	23874
2455200.31029	0.00019	23941
2455515.38459	0.00024	26299
2455520.32865	0.00038	26336
2455533.42346	0.00028	26434
2455889.38551	0.00036	29098
2455891.39036	0.00024	29113
2455893.39432	0.00019	29128
2456267.39501	0.00019	31927
2456271.40415	0.00015	31957
2456298.39531	0.00018	32159
2456725.30918	0.00035	35354
2457017.40117	0.00013	37540
2457020.34099	0.00034	37562
2457442.31106	0.00011	40720
2457443.38007	0.00017	40728
2458099.31749	0.00018	45637
2458103.45938	0.00016	45668
2458106.26552	0.00040	45689
2458444.32328	0.00034	48219
2458477.32701	0.00022	48466
2458493.36113	0.00005	48586
2458784.38450	0.00022	50764
2458806.29770	0.00031	50928
2458817.25411	0.00029	51010
2459149.43247	0.00024	53496
2459157.44964	0.00016	53556
2459159.32000	0.00023	53570

Table 3.2. Eclipse times, errors and cycle numbers for SW Sex observed and measured by the author in this study.

<i>Eclipse time (HJD)</i>	<i>Error (d)</i>	<i>Cycle Number</i>
2454185.43702	0.00044	72965
2454186.38145	0.00029	72972
2454553.41407	0.00048	75692
2454564.34410	0.00020	75773
2454906.41325	0.00019	78308
2454907.49269	0.00019	78316
2455260.35696	0.00018	80931
2455278.43821	0.00012	81065
2455630.35814	0.00026	83673
2455660.44910	0.00014	83896
2455662.33853	0.00028	83910
2455992.39775	0.00022	86356
2456005.48662	0.00010	86453
2456008.45550	0.00018	86475
2456343.50779	0.00012	88958
2456354.43764	0.00013	89039
2456356.46180	0.00016	89054
2456728.35219	0.00019	91810
2456739.41702	0.00013	91892
2457118.45908	0.00019	94701
2457119.40351	0.00010	94708
2457461.33764	0.00017	97242
2457462.41694	0.00015	97250
2457465.38568	0.00024	97272
2457833.36314	0.00014	99999
2457835.38696	0.00014	100014
2457836.33134	0.00026	100021
2457837.41089	0.00015	100029
2457862.37464	0.00018	100214
2458191.48919	0.00009	102653
2458212.40447	0.00013	102808
2458214.42856	0.00010	102823
2458567.42678	0.00008	105439
2458571.33929	0.00016	105468
2458575.38787	0.00011	105498
2458584.42857	0.00009	105565
2458585.37339	0.00014	105572
2458931.35406	0.00015	108136
2458932.43393	0.00010	108144
2458933.37801	0.00029	108151
2459281.38341	0.00015	110730
2459282.46286	0.00017	110738
2459291.36857	0.00011	110804
2459677.42673	0.00014	113665
2459683.36420	0.00025	113709
2459685.38844	0.00021	113724
2460052.42102	0.00008	116444
2460054.44524	0.00011	116459
2460064.43065	0.00028	116533

Table 3.3. Eclipse times, errors and cycle numbers for DW UMa observed and measured by the author in this study.

<i>Eclipse time (HJD)</i>	<i>Error (d)</i>	<i>Cycle Number</i>
2454181.41978	0.00019	58214
2454185.38111	0.00029	58243
2454224.45051	0.00043	58529
2454473.34780	0.00038	60351
2454564.46466	0.00020	61018
2454580.44785	0.00033	61135
2454580.58433	0.00026	61136
2454588.37104	0.00028	61193
2454588.50711	0.00019	61194
2454593.42488	0.00022	61230
2454596.43092	0.00033	61252
2454884.39723	0.00024	63360
2454892.32009	0.00025	63418
2455239.30026	0.00021	65958
2455263.34322	0.00014	66134
2455270.31000	0.00013	66185
2455278.37037	0.00017	66244
2455627.39978	0.00017	68799
2455628.35604	0.00020	68806
2455629.31205	0.00029	68813
2455991.45632	0.00028	71464
2456029.43254	0.00029	71742
2456033.39472	0.00022	71771
2456088.44663	0.00035	72174
2456382.42440	0.00027	74326
2456384.47293	0.00013	74341
2456399.36316	0.00039	74450
2456413.43361	0.00024	74553
2456728.44826	0.00015	76859
2456739.37663	0.00011	76939
2457020.37615	0.00026	78996
2457021.46907	0.00019	79004
2457075.42859	0.00021	79399
2457106.43843	0.00010	79626
2457108.35065	0.00012	79640
2457108.48716	0.00020	79641
2458174.42888	0.00017	87444
2458188.36286	0.00021	87546
2458191.36841	0.00019	87568
2458227.43235	0.00020	87832
2458231.39341	0.00016	87861
2458234.39877	0.00035	87883
2458539.44267	0.00039	90116
2458540.39817	0.00023	90123
2458541.35463	0.00015	90130
2458571.40737	0.00012	90350
2458585.34131	0.00025	90452
2458593.40129	0.00019	90511
2458855.41318	0.00034	92429
2458861.42412	0.00031	92473
2458868.39096	0.00013	92524
2458948.44193	0.00028	93110
2459258.40274	0.00058	95379
2459268.37535	0.00016	95452
2459272.33702	0.00017	95481
2459597.32418	0.00032	97860
2459599.37245	0.00018	97875
2459600.32970	0.00029	97882
2459968.34763	0.00022	100576
2459975.31458	0.00022	100627
2459989.38528	0.00017	100730

Table 3.4. Eclipse times, errors and cycle numbers for HS0129+2933 observed and measured by the author in this study.

<i>Eclipse time (HJD)</i>	<i>Error (d)</i>	<i>Cycle Number</i>
2454061.46332	0.00014	10892
2454081.29219	0.00016	11034
2454086.45848	0.00008	11071
2455106.37036	0.00038	18375
2455188.47729	0.00030	18963
2455191.27007	0.00019	18983
2455460.49099	0.00013	20911
2455533.38206	0.00022	21433
2455827.45860	0.00014	23539
2455835.41776	0.00016	23596
2455836.39518	0.00010	23603
2456200.43010	0.00037	26210
2456215.37178	0.00019	26317
2456237.29459	0.00022	26474
2456527.46137	0.00028	28552
2456611.38335	0.00017	29153
2456901.41023	0.00021	31230
2456904.48240	0.00024	31252
2457258.46323	0.00012	33787
2457276.47630	0.00017	33916
2457624.45255	0.00033	36408
2457631.43448	0.00018	36458
2458029.40123	0.00026	39308
2458054.39650	0.00011	39487
2458056.35143	0.00013	39501
2458362.43603	0.00029	41693
2458363.41333	0.00016	41700
2458388.40829	0.00022	41879
2458721.44286	0.00017	44264
2458741.41060	0.00012	44407
2458759.42431	0.00004	44536
2458773.38793	0.00031	44636
2458906.32283	0.00025	45588
2459105.44446	0.00018	47014
2459106.42148	0.00027	47021
2459107.39970	0.00014	47028
2459523.37876	0.00015	50007
2459526.31147	0.00011	50028
2459541.39281	0.00015	50136
2459914.36388	0.00021	52807
2459921.34628	0.00025	52857
2459928.32801	0.00018	52907

Table 3.5. Eclipse times, errors and cycle numbers for V1315 Aql observed and measured by the author in this study.

<i>Eclipse time (HJD)</i>	<i>Error (d)</i>	<i>Cycle Number</i>
2454272.50437	0.00018	59916
2454306.44865	0.00027	60159
2454313.43262	0.00072	60209
2454651.48330	0.00048	62629
2454670.48100	0.00046	62765
2454810.31097	0.00082	63766
2455004.47952	0.00029	65156
2455006.43480	0.00049	65170
2455038.42351	0.00055	65399
2455052.39293	0.00070	65499
2455463.36184	0.00047	68441
2455464.33978	0.00036	68448
2455490.32143	0.00026	68634
2455777.38468	0.00040	70689
2455783.39087	0.00040	70732
2455903.24546	0.00047	71590
2456131.49866	0.00042	73224
2456149.51903	0.00035	73353
2456150.49660	0.00023	73360
2456215.31256	0.00061	73824
2456446.49995	0.00064	75479
2456453.48465	0.00056	75529
2456478.48866	0.00025	75708
2456838.47024	0.00025	78285
2456845.45485	0.00023	78335
2456895.46344	0.00033	78693
2457177.49766	0.00035	80712
2457184.48150	0.00042	80762
2457203.47971	0.00026	80898
2457293.30101	0.00042	81541
2457303.35804	0.00028	81613
2457563.46136	0.00028	83475
2457587.48793	0.00021	83647
2457590.42138	0.00019	83668
2457960.46038	0.00063	86317
2457971.49598	0.00025	86396
2457978.48056	0.00023	86446
2458294.45908	0.00057	88708
2458295.43676	0.00018	88715
2458314.43516	0.00027	88851
2458655.41791	0.00044	91292
2458665.47589	0.00053	91364
2458666.45373	0.00030	91371
2459024.47947	0.00032	93934
2459025.45740	0.00032	93941
2459033.41968	0.00041	93998
2459365.46204	0.00035	96375
2459366.44091	0.00031	96382
2459379.43190	0.00044	96475
2459744.44107	0.00062	99088
2459756.45506	0.00023	99174
2459757.43293	0.00059	99181

Table 3.6. Eclipse times, errors and cycle numbers for PX And observed and measured by the author in this study.

<i>Eclipse time (HJD)</i>	<i>Error (d)</i>	<i>Cycle Number</i>
2454318.44729	0.00051	34708
2454319.47234	0.00046	34715
2454325.47261	0.00036	34756
2454448.40773	0.00061	35596
2454473.28943	0.00051	35766
2454503.29163	0.00022	35971
2454761.45718	0.00049	37735
2454770.38547	0.00069	37796
2455064.40680	0.00108	39805
2455066.45577	0.00069	39819
2455173.29503	0.00032	40549
2455186.32065	0.00020	40638
2455188.36884	0.00125	40652
2455191.29553	0.00055	40672
2455201.24653	0.00014	40740
2455460.43876	0.00028	42511
2455495.26963	0.00061	42749
2455515.46733	0.00025	42887
2455795.43984	0.00024	44800
2455819.44115	0.00069	44964
2455823.39248	0.00044	44991
2455901.25250	0.00064	45523
2456149.46690	0.00038	47219
2456159.41895	0.00035	47287
2456215.32501	0.00053	47669
2456512.42294	0.00048	49699
2456518.42177	0.00083	49740
2456609.45353	0.00040	50362
2456611.35720	0.00069	50375
2456908.45223	0.00028	52405
2456922.35622	0.00047	52500
2457271.40745	0.00041	54885
2457275.50498	0.00026	54913
2457615.48272	0.00042	57236
2457624.41054	0.00047	57297
2457994.38914	0.00082	59825
2457996.43794	0.00026	59839
2457997.46265	0.00064	59846
2458362.46761	0.00038	62340
2458379.44407	0.00025	62456
2458759.37448	0.00018	65052
2458806.35537	0.00021	65373
2458817.33089	0.00013	65448
2459114.42636	0.00047	67478
2459148.38126	0.00068	67710

Table 3.7. Eclipse times, errors and cycle numbers for HS 0455+8315 observed and measured by the author in this study.

<i>Eclipse time (HJD)</i>	<i>Error (d)</i>	<i>Cycle Number</i>
2454061.40139	0.00016	14807
2454063.48351	0.00020	14821
2454078.35643	0.00014	14921
2454112.41335	0.00017	15150
2454114.49593	0.00023	15164
2454115.38831	0.00017	15170
2454895.44552	0.00018	20415
2454906.45070	0.00013	20489
2454907.34318	0.00026	20495
2455065.43666	0.00029	21558
2455495.39753	0.00032	24449
2455519.49112	0.00017	24611
2455526.48082	0.00018	24658
2455835.38030	0.00021	26735
2455850.40114	0.00018	26836
2456271.43853	0.00015	29667
2456274.41353	0.00029	29687
2456294.34258	0.00019	29821
2456538.39879	0.00012	31462
2456903.36710	0.00014	33916
2456908.42377	0.00027	33950
2457276.36680	0.00018	36424
2457291.38805	0.00021	36525
2457594.48734	0.00024	38563
2457609.50881	0.00016	38664
2458038.42837	0.00022	41548
2458039.32057	0.00017	41554
2458042.29484	0.00019	41574
2458385.40088	0.00027	43881
2458386.44190	0.00004	43888
2458719.43614	0.00012	46127
2458721.36860	0.00023	46140
2458784.42820	0.00020	46564
2458806.43966	0.00018	46712
2458911.43828	0.00015	47418
2458925.41820	0.00014	47512
2459041.42251	0.00017	48292
2459053.46929	0.00025	48373
2459056.44407	0.00010	48393
2459110.43117	0.00022	48756
2459117.42066	0.00011	48803
2459389.43726	0.00014	50632
2459414.42257	0.00010	50800
2459415.46405	0.00014	50807

Table 3.8. Eclipse times, errors and cycle numbers for HS 0220+0603 observed and measured by the author in this study.

<i>Eclipse time (HJD)</i>	<i>Error (d)</i>	<i>Cycle Number</i>
2454061.32109	0.00048	10038
2454081.31479	0.00032	10172
2454081.46403	0.00018	10173
2454086.38783	0.00026	10206
2455156.35608	0.00028	17377
2455188.43603	0.00027	17592
2455200.37262	0.00034	17672
2455490.43180	0.00028	19616
2455515.34977	0.00031	19783
2455533.40410	0.00029	19904
2455867.48013	0.00024	22143
2455884.48964	0.00012	22257
2456249.45127	0.00022	24703
2456250.49598	0.00015	24710
2456266.46118	0.00022	24817
2456609.34044	0.00042	27115
2456619.33720	0.00028	27182
2456955.50247	0.00033	29435
2456985.34355	0.00024	29635
2457354.48328	0.00027	32109
2457403.27389	0.00013	32436
2457407.30240	0.00016	32463
2457684.38159	0.00023	34320
2457698.40661	0.00021	34414
2458054.41601	0.00022	36800
2458082.31770	0.00022	36987
2458477.27022	0.00022	39634
2458492.34036	0.00031	39735
2458817.46349	0.00020	41914
2458819.40361	0.00011	41927
2458822.38782	0.00018	41947
2459158.40349	0.00019	44199
2459176.45724	0.00022	44320
2459189.43843	0.00018	44407
2459584.39131	0.00034	47054
2459597.37209	0.00038	47141
2459870.42209	0.00032	48971

Table 3.9. Eclipse times, errors and cycle numbers for BP Lyn observed and measured by the author in this study.

<i>Eclipse time (HJD)</i>	<i>Error (d)</i>	<i>Cycle Number</i>
2454186.44462	0.00069	41257
2454891.36892	0.00095	45870
2454906.49781	0.00084	45969
2455239.32473	0.00058	48147
2455260.41122	0.00042	48285
2455263.31415	0.00049	48304
2455571.38461	0.00074	50320
2455594.30701	0.00042	50470
2455619.52087	0.00059	50635
2455914.44759	0.00041	52565
2455930.34125	0.00063	52669
2455932.32762	0.00066	52682
2455942.41314	0.00039	52748
2455991.31277	0.00055	53068
2456016.37415	0.00052	53232
2456338.34928	0.00069	55339
2456343.39349	0.00056	55372
2456355.31121	0.00039	55450
2456356.38067	0.00034	55457
2456410.47808	0.00063	55811
2456415.36759	0.00065	55843
2456684.31780	0.00044	57603
2456728.32764	0.00126	57891
2457021.42236	0.00055	59809
2457059.32139	0.00083	60057
2457062.37785	0.00044	60077
2457433.40551	0.00051	62505
2457447.31156	0.00062	62596
2457455.41132	0.00026	62649
2457758.43751	0.00046	64632
2457778.30406	0.00037	64762
2458137.41551	0.00031	67112
2458161.40539	0.00031	67269
2458162.32198	0.00042	67275
2458163.39102	0.00040	67282
2458514.40265	0.00055	69579
2458517.30581	0.00051	69598
2458526.32134	0.00072	69657
2458539.31249	0.00049	69742
2458864.34320	0.00073	71869
2458886.34755	0.00040	72013
2458925.46891	0.00045	72269
2459240.41430	0.00037	74330
2459258.44656	0.00062	74448
2459271.43627	0.00051	74533

Table 3.10. Eclipse times, errors and cycle numbers for BH Lyn observed and measured by the author in this study.

<i>Eclipse time (HJD)</i>	<i>Error (d)</i>	<i>Cycle Number</i>
2454181.48914	0.00029	44915
2454186.32132	0.00042	44946
2454199.41436	0.00053	45030
2454482.32954	0.00048	46845
2454834.45234	0.00046	49104
2454884.33284	0.00052	49424
2455247.36666	0.00027	51753
2455260.46000	0.00033	51837
2455267.31793	0.00059	51881
2455594.34608	0.00035	53979
2455628.32676	0.00041	54197
2455670.41251	0.00040	54467
2455675.40111	0.00031	54499
2455895.34197	0.00038	55910
2455902.35570	0.00039	55955
2455941.32605	0.00040	56205
2455992.45237	0.00076	56533
2455994.32276	0.00053	56545
2455994.47949	0.00087	56546
2456028.45927	0.00021	56764
2456298.43632	0.00040	58496
2456356.42123	0.00032	58868
2456382.45272	0.00022	59035
2456699.34816	0.00027	61068
2456707.45398	0.00027	61120
2456726.47051	0.00038	61242
2457017.33447	0.00048	63108
2457020.45224	0.00043	63128
2457021.38791	0.00056	63134
2457433.36610	0.00032	65777
2457443.34252	0.00031	65841
2457460.48838	0.00021	65951
2457721.42424	0.00040	67625
2457727.34740	0.00043	67663
2458155.38234	0.00031	70409
2458163.33224	0.00019	70460
2458172.37306	0.00035	70518
2458840.45547	0.00035	74804
2458864.30434	0.00028	74957
2458868.35774	0.00038	74983
2459221.41548	0.00019	77248
2459238.40565	0.00017	77357
2459256.33224	0.00016	77472

Table 3.11. Eclipse times, errors and cycle numbers for LX Ser observed and measured by the author in this study.

<i>Eclipse time (HJD)</i>	<i>Error (d)</i>	<i>Cycle Number</i>
2454316.41420	0.00032	63266
2454628.52570	0.00023	65236
2454976.44297	0.00038	67432
2454994.50414	0.00026	67546
2455001.47525	0.00033	67590
2455037.43960	0.00020	67817
2455662.45627	0.00040	71762
2455663.40637	0.00045	71768
2455672.43730	0.00041	71825
2455778.42860	0.00031	72494
2456028.43528	0.00029	74072
2456076.44023	0.00042	74375
2456088.48102	0.00025	74451
2456384.43183	0.00028	76319
2456403.44388	0.00026	76439
2456410.41513	0.00047	76483
2456412.47433	0.00021	76496
2456782.41518	0.00010	78831
2456792.39591	0.00050	78894
2456798.41635	0.00018	78932
2457134.45163	0.00014	81053
2457159.48411	0.00019	81211
2457163.44478	0.00017	81236
2457491.40048	0.00055	83306
2457496.47045	0.00039	83338
2457506.45164	0.00033	83401
2457900.47370	0.00029	85888
2457901.42457	0.00029	85894
2457939.44889	0.00027	86134
2458227.47854	0.00022	87952
2458228.42935	0.00028	87958
2458241.42094	0.00033	88040
2458246.49055	0.00023	88072
2458593.45853	0.00026	90262
2458594.40834	0.00031	90268
2458599.47913	0.00019	90300
2458603.43930	0.00015	90325
2458943.43549	0.00035	92471
2458946.44578	0.00033	92490
2458949.45551	0.00039	92509
2459341.41767	0.00021	94983
2459350.44820	0.00011	95040
2459354.40902	0.00033	95065
2459704.38657	0.00024	97274
2459713.41715	0.00044	97331
2459744.47026	0.00029	97527

Table 3.12. Eclipse times, errors and cycle numbers for UU Aqr observed and measured by the author in this study.

<i>Eclipse time (HJD)</i>	<i>Error (d)</i>	<i>Cycle Number</i>
2454323.44995	0.00046	48760
2454357.47405	0.00027	48968
2454365.48955	0.00036	49017
2454728.47437	0.00051	51236
2454735.34486	0.00034	51278
2454736.32601	0.00056	51284
2454789.32574	0.00032	51608
2455038.45994	0.00069	53131
2455059.39716	0.00052	53259
2455106.34585	0.00043	53546
2455469.49424	0.00052	55766
2455490.26865	0.00048	55893
2455778.49715	0.00019	57655
2455795.50952	0.00019	57759
2455893.33048	0.00019	58357
2456159.47572	0.00030	59984
2456160.45716	0.00033	59990
2456162.42044	0.00044	60002
2456215.42071	0.00018	60326
2456512.48351	0.00045	62142
2456523.44298	0.00024	62209
2456532.43936	0.00066	62264
2456611.28481	0.00045	62746
2456612.26681	0.00033	62752
2456893.46177	0.00016	64471
2456903.44070	0.00038	64532
2456904.42104	0.00036	64538
2457258.40900	0.00022	66702
2457262.49817	0.00020	66727
2457275.42161	0.00012	66806
2457609.45204	0.00021	68848
2457617.46778	0.00040	68897
2457642.49568	0.00040	69050
2457979.47132	0.00035	71110
2457989.44973	0.00043	71171
2457993.37551	0.00026	71195
2458352.43417	0.00030	73390
2458360.44924	0.00025	73439
2458362.41308	0.00018	73451
2458363.39380	0.00024	73457
2458766.45546	0.00027	75921
2458784.28619	0.00018	76030
2458799.33537	0.00016	76122
2459102.44929	0.00024	77975
2459106.37518	0.00017	77999
2459107.35642	0.00036	78005
2459476.39397	0.00025	80261
2459478.35668	0.00047	80273
2459498.31321	0.00043	80395
2459499.29486	0.00029	80401
2459799.46523	0.00030	82236
2459859.33507	0.00055	82602
2459902.35724	0.00014	82865

Table 4. Eclipse times, errors and cycle numbers for LX Ser measured by the author from observations by Cook and Dvorak in the AAVSO International Database.

<i>Eclipse time (HJD)</i>	<i>Error (d)</i>	<i>Cycle Number</i>	<i>Observer</i>	<i>Eclipse time (HJD)</i>	<i>Error (d)</i>	<i>Cycle Number</i>	<i>Observer</i>
2452777.87523	0.00050	53555	Cook	2458192.94006	0.00020	87734	Dvorak
2452778.82598	0.00056	53561	Cook	2458193.89137	0.00042	87740	Dvorak
2452779.77652	0.00072	53567	Cook	2458220.82416	0.00025	87910	Dvorak
2452779.93474	0.00057	53568	Cook	2458227.79532	0.00032	87954	Dvorak
2452780.88542	0.00044	53574	Cook	2458233.81608	0.00042	87992	Dvorak
2452781.83604	0.00049	53580	Cook	2458239.83639	0.00045	88030	Dvorak
2452782.78676	0.00050	53586	Cook	2458242.84637	0.00036	88049	Dvorak
2452782.94528	0.00051	53587	Cook	2458272.63221	0.00031	88237	Dvorak
2452786.74760	0.00036	53611	Cook	2458589.65567	0.00034	90238	Dvorak
2452786.90593	0.00022	53612	Cook	2458966.72465	0.00027	92618	Dvorak
2452787.85672	0.00041	53618	Cook	2459271.86577	0.00043	94544	Dvorak
2457882.73016	0.00052	85776	Dvorak	2459358.68647	0.00030	95092	Dvorak
2457889.70010	0.00037	85820	Dvorak	2459363.59809	0.00021	95123	Dvorak
2457899.68152	0.00027	85883	Dvorak	2459364.70675	0.00017	95130	Dvorak
2458167.90800	0.00032	87576	Dvorak	2459375.63919	0.00029	95199	Dvorak
2458181.85027	0.00035	87664	Dvorak	2459624.85361	0.00032	96772	Dvorak
2458187.87047	0.00021	87702	Dvorak	2459625.96292	0.00050	96779	Dvorak
2458191.83129	0.00031	87727	Dvorak	2459744.47026	0.00029	97527	Dvorak

Table 5. Sources of published eclipse times.

<i>Star Name</i>	<i>Sources of published eclipse times</i>
HS 0728+6738 = V482 Cam SW Sex = PG 1012-029 DW UMa = PG1030+590	Rodriguez-Gil <i>et al.</i> (2004) Penning <i>et al.</i> (1984), Ashoka <i>et al.</i> (1994), Dhillon <i>et al.</i> (1997), Groot <i>et al.</i> (2001), Fang <i>et al.</i> (2020), one issue of BVSOLJ Shafter <i>et al.</i> (1988), Dhillon <i>et al.</i> (1994), Biró (2000), Stanishev <i>et al.</i> (2004), Dhillon <i>et al.</i> (2013), Boyd <i>et al.</i> (2017) (including observations from contributors to the Centre for Backyard Astrophysics), several issues of IBVS, BVSOLJ, OEJV
HS 0129+2933 = TT Tri V1315 Aql	Warren <i>et al.</i> (2006), Rodriguez-Gil <i>et al.</i> (2007), Han <i>et al.</i> (2018) Downes <i>et al.</i> (1986), Dhillon <i>et al.</i> (1991), Rutten <i>et al.</i> (1992), Hellier (1996), Papadaki <i>et al.</i> (2009), Fang and Qian (2021), a series of eclipse times by Cook published in <i>Observed Minima Times of Eclipsing Binaries, No 10</i> (Baldwin and Samolyk 2005)
PX And = PG0027+260 HS 0455+8315 HS 0220+0603 BP Lyn = PG0859+415 BH Lyn = PG0818+513 LX Ser = Stepanyan's Star	Hellier and Robinson (1994), Stanishev <i>et al.</i> (2002), Han <i>et al.</i> (2018), several issues of IBVS Rodriguez-Gil <i>et al.</i> (2007) Rodriguez-Gil <i>et al.</i> (2007) Grauer <i>et al.</i> (1994), Still (1996), Han <i>et al.</i> (2018) Dhillon <i>et al.</i> (1992), Hoard and Szkody (1997), Stanishev <i>et al.</i> (2006), several issues of OEJV Horne (1980), Africano and Klimke (1981), Young <i>et al.</i> (1981), Rutten <i>et al.</i> (1992), Li (2017), several issues of IBVS, BVSOLJ and OEJV
UU Aqr V1776 Cyg = Lanning 90 RW Tri	Baptista <i>et al.</i> (1994), Han <i>et al.</i> (2018), several issues of BVSOLJ, IBVS and OEJV Garnavich <i>et al.</i> (1990) Walker (1963), Africano <i>et al.</i> (1978), Robinson <i>et al.</i> (1991), Rutten <i>et al.</i> (1992), Smak (1995), Subebikova (2020), several issues of IBVS, OEJV and BVSOLJ
1RXS J064434.5+334451 AC Cnc	Sing <i>et al.</i> (2007), Green (2008), Hernandez Santisteban (2017), Shafter and Bautista (2021) Yamasaki <i>et al.</i> (1983), Schlegel <i>et al.</i> (1984), Zhang <i>et al.</i> (1987), Thoroughgood <i>et al.</i> (2004), Qian <i>et al.</i> (2007), Bruch (2022), several issues of OEJV and IBVS
V363 Aur = Lanning 10 BT Mon	Horne <i>et al.</i> (1982), Schlegel <i>et al.</i> (1986), Rutten <i>et al.</i> (1992), Thoroughgood <i>et al.</i> (2004), one issue of BVSOLJ Robinson <i>et al.</i> (1982), Seitter (1984), Smith <i>et al.</i> (1998)

IBVS = *Information Bulletin on Variable Stars*: <https://konkoly.hu/ibvs/>; BVSOLJ = *Bulletin of the Variable Star Observers League in Japan*: <http://vsolj.cetus-net.org/>;
OEJV = *Open European Journal on Variable Stars*: <https://oejv.physics.muni.cz/>

Table 6. Weighted linear ephemerides for each star computed with all available data except in the case of SW Sex where there was a large change around 2017 and separate ephemerides are given for before and after this change. E is the cycle number.

<i>Star Name</i>	<i>Weighted Linear Ephemeris</i>
HS 0728+6738 = V482 Cam	2452001.32754(8) + 0.133619431(2) * E
SW Sex = PG 1012-029 (up to 2017)	2444339.6502(2) + 0.134938480(2) * E
SW Sex = PG 1012-029 (after 2017)	2444339.689(2) + 0.13493809(2) * E
DW UMa = PG1030+590	2446229.00633(8) + 0.136606541(1) * E
HS 0129+2933 = TT Tri	2452540.5335(2) + 0.139637390(7) * E
V1315 Aql	2445902.8387(2) + 0.139689996(2) * E
PX And = PG0027+260	2449238.8368(2) + 0.146352742(4) * E
HS 0455+8315	2451859.2458(2) + 0.148723946(5) * E
HS 0220+0603	2452563.57441(9) + 0.149207655(3) * E
BP Lyn = PG0859+415	2447881.8572(4) + 0.152812554(7) * E
BH Lyn = PG0818+513	2447180.3343(2) + 0.155875642(3) * E
LX Ser = Stepanyan's Star	2444293.0227(2) + 0.158432503(2) * E
UU Aqr	2446347.2670(2) + 0.163580423(3) * E
V1776 Cyg = Lanning 90	2447048.7932(3) + 0.164738652(5) * E
RW Tri	2441129.3634(4) + 0.231883245(5) * E
IRXS J064434.5+334451	2453403.7611(3) + 0.26937438(2) * E
AC Cnc	2444290.3103(3) + 0.300477307(7) * E
V363 Aur = Lanning 10	2444557.981(2) + 0.32124074(6) * E
BT Mon	2443491.7225(9) + 0.33381330(2) * E

Table 7. Weighted quadratic ephemerides and mean rates of period change for stars showing evidence of either an increasing or decreasing orbital period. E is the cycle number.

<i>Star Name</i>	<i>Weighted Quadratic Ephemeris</i>	<i>Mean Rate of Period Change (msec/year)</i>
HS 0728+6738 = V482 Cam	2452001.3273(1) + 0.133619451(8) * E - 3(1)10 ⁻¹³ * E ²	-0.16(6)
DW UMa = PG1030+590	2446229.0069(2) + 0.136606520(7) * E + 1.7(5)10 ⁻¹³ * E ²	0.08(3)
HS 0129+2933 = TT Tri	2452540.5309(2) + 0.13963764(2) * E - 4.2(3)10 ⁻¹² * E ²	-1.9(2)
V1315 Aql	2445902.8408(1) + 0.139689913(4) * E + 6.8(3)10 ⁻¹³ * E ²	0.31(2)
PX And = PG0027+260	2449238.8366(2) + 0.14635275(1) * E - 1(1)10 ⁻¹³ * E ²	-0.06(6)
HS 0455+8315	2451859.2476(5) + 0.14872382(3) * E + 1.9(5)10 ⁻¹² * E ²	0.8(2)
HS 0220+0603	2452563.57406(7) + 0.149207716(7) * E - 1.4(2) 10 ⁻¹² * E ²	-0.58(6)
BP Lyn = PG0859+415	2447881.8584(4) + 0.15281244(2) * E + 1.5(3)10 ⁻¹² * E ²	0.6(1)
BH Lyn = PG0818+513	2447180.3331(2) + 0.155875697(3) * E - 5.51(3)10 ⁻¹³ * E ²	-0.22(1)
UU Aqr	2446347.2656(1) + 0.163580565(8) * E - 1.70(9)10 ⁻¹² * E ²	-0.66(4)
V1776 Cyg = Lanning 90	2447048.7928(3) + 0.16473869(2) * E - 5(2)10 ⁻¹³ * E ²	-0.19(8)
IRXS J064434.5+334451	2453403.7596(3) + 0.26937469(5) * E - 1.2(2)10 ⁻¹¹ * E ²	-2.8(5)
V363 Aur = Lanning 10	2444557.9493(5) + 0.32124275(2) * E - 3.05(2)10 ⁻¹¹ * E ²	-5.98(4)
BT Mon	2443491.7162(4) + 0.33381392(1) * E - 1.127(8)10 ⁻¹¹ * E ²	-2.13(2)

Table 8. Parameters of sinusoidal fits relative to a linear ephemeris.

<i>Star Name</i>	<i>Period of Sinusoidal Variation (year)</i>	<i>Half Amplitude of Sinusoidal Variation (sec)</i>
SW Sex = PG 1012-029 (up to 2017)	33 (2)	46 (6)
LX Ser = Stepanyan's Star	13.5 (2)	55 (4)
RW Tri up (up to 2018)	44.3 (7)	191 (7)
AC Cnc	37.8 (7)	134 (14)

Table 9. Parameters of sinusoidal fits relative to a quadratic ephemeris.

<i>Star Name</i>	<i>Period of Sinusoidal Variation (year)</i>	<i>Half Amplitude of Sinusoidal Variation (sec)</i>
DW UMa = PG1030+590	14.4 (3)	38 (1)
HS 0129+2933 = TT Tri	13.0 (4)	47 (6)
IRXS J064434.5+334451	6.2 (2)	87 (10)

5. O–C diagrams

In these O–C diagrams, data from the published literature or derived from observations in the AAVSO International Database are shown in black while eclipse times measured by the author are shown in red. Linear ephemerides are shown dotted in black, quadratic ephemerides dotted in magenta, and sinusoidal fits dotted in green. The passing years are marked above each diagram. O–C diagrams with similar apparent behavior are grouped together. To achieve a degree of consistency between these diagrams, we have used the same scale on the O–C axis except where the range of the data is significantly larger. It is worth stating explicitly that including these fits in the O–C diagrams is a subjective exercise which yields parameters that can be quantified but does not imply a physical interpretation. The O–C diagrams are described in five groups.

HS 0728+6738 = V482 Cam, *PX And = PG0027+260*, *HS 0220+0603*, *BH Lyn = PG0818+513*, *V1776 Cyg = Lanning 90* These stars show predominantly linear behavior with weak evidence of decreasing orbital period. Their O–C diagrams with linear and quadratic ephemerides are shown in Figure 2 and parameters of the quadratic ephemerides are given in Table 7.

HS 0129+2933 = TT Tri, *UU Aqr*, *1RXS J064434.5+334451*, *V363 Aur = Lanning 10*, *BT Mon* These stars show stronger evidence of decreasing orbital periods. Their O–C diagrams with linear and quadratic ephemerides are shown in Figure 3 and parameters of the quadratic ephemerides are given in Table 7.

DW UMa = PG1030+590, *V1315 Aql*, *HS0455+8315*, *BP Lyn = PG0859+415* These stars show evidence of increasing orbital periods. Their O–C diagrams with linear and quadratic ephemerides are shown in Figure 4 and parameters of the quadratic ephemerides are given in Table 7.

SW Sex = PG 1012-029, *LX Ser = Stepanyan's Star*, *RW Tri*, *AC Cnc* These stars show evidence of sinusoidal variation in their orbital periods relative to a linear ephemeris. Figure 5 shows their O–C diagrams with sinusoidal fits relative to a linear ephemeris and Table 8 gives parameters of these sinusoidal fits.

Stars also showing evidence of more complex behavior In addition to their behavior described above, DW UMa, HS0129+2933 and 1RXS J064434.5+334451 also show evidence of sinusoidal variation in their orbital periods relative to a quadratic ephemeris. Figure 6 shows their O–C diagrams with sinusoidal fits relative to a quadratic ephemeris. Table 9 gives parameters of these sinusoidal fits. DW UMa now appears to be diverging from this sinusoidal pattern.

Figure 5 shows that both SW Sex and RW Tri recently experienced large decreases in their orbital periods.

Prior to 2017 (cycle ~ 100000) the mean orbital period of SW Sex over the previous 37 years had been 0.134938480(2) d with relatively weak sinusoidal modulation. During 2017 this reduced to 0.13493809(2) d, a decrease of 34 msec and a proportional change of -2.9×10^{-6} .

Prior to 2018 (cycle ~ 74000) the mean orbital period of RW Tri over the previous 15 years had been 0.231883411(6) d with relatively strong sinusoidal modulation. Within a few months this changed and the mean orbital period since 2018 has been 0.23188288(6) d, a decrease of 46 msec and a proportional change of -2.3×10^{-6} .

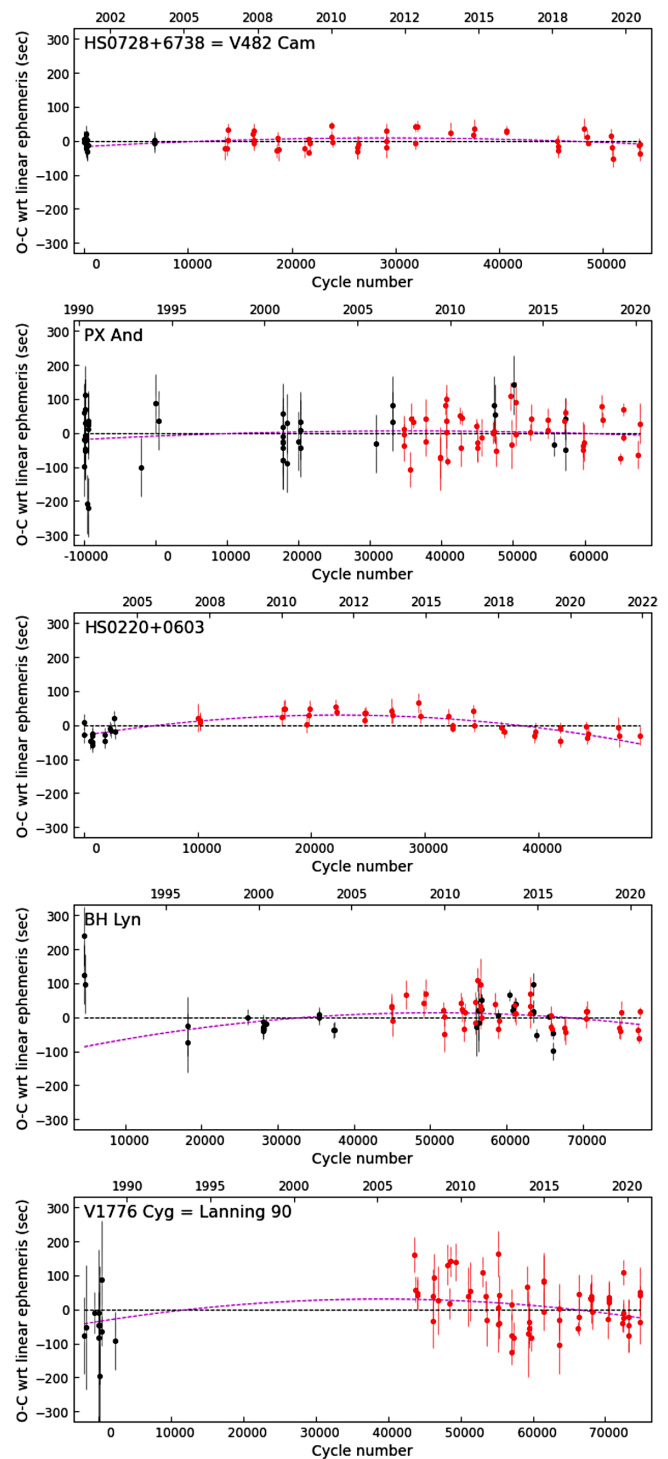


Figure 2. O–C diagrams with linear and quadratic ephemerides for stars showing weak evidence of decreasing orbital period. Data from the published literature or derived from observations in the AAVSO International Database are shown in black while eclipse times measured by the author are shown in red. Linear ephemerides are shown dotted in black, quadratic fits dotted in magenta.

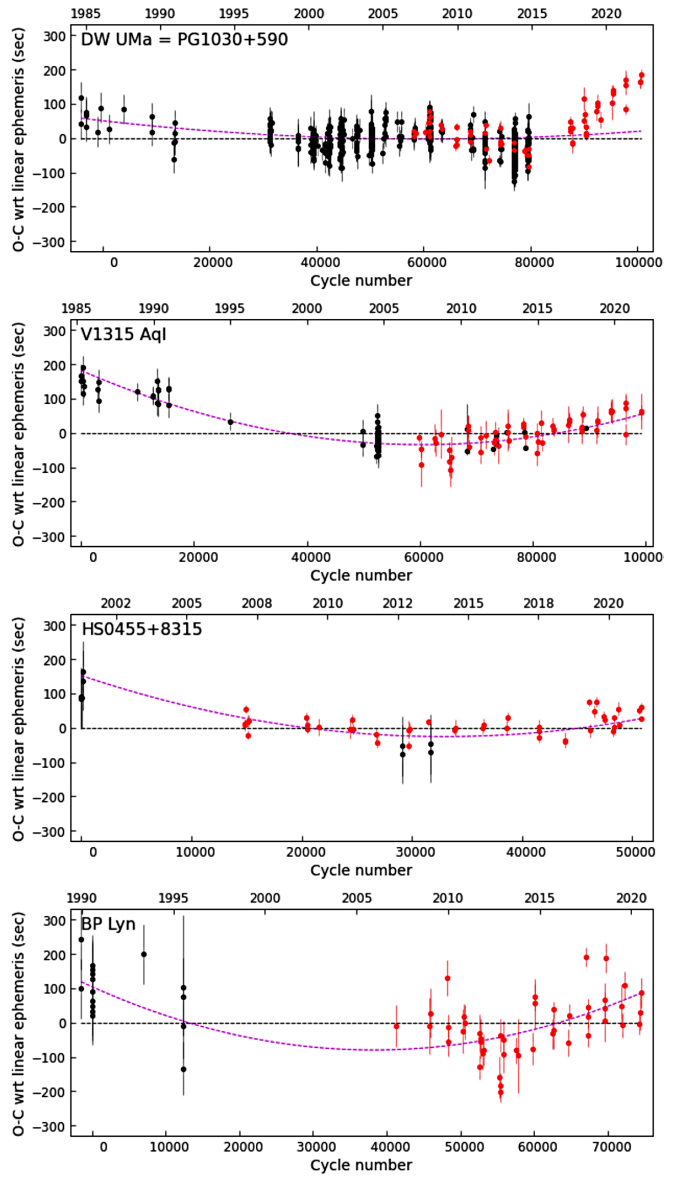
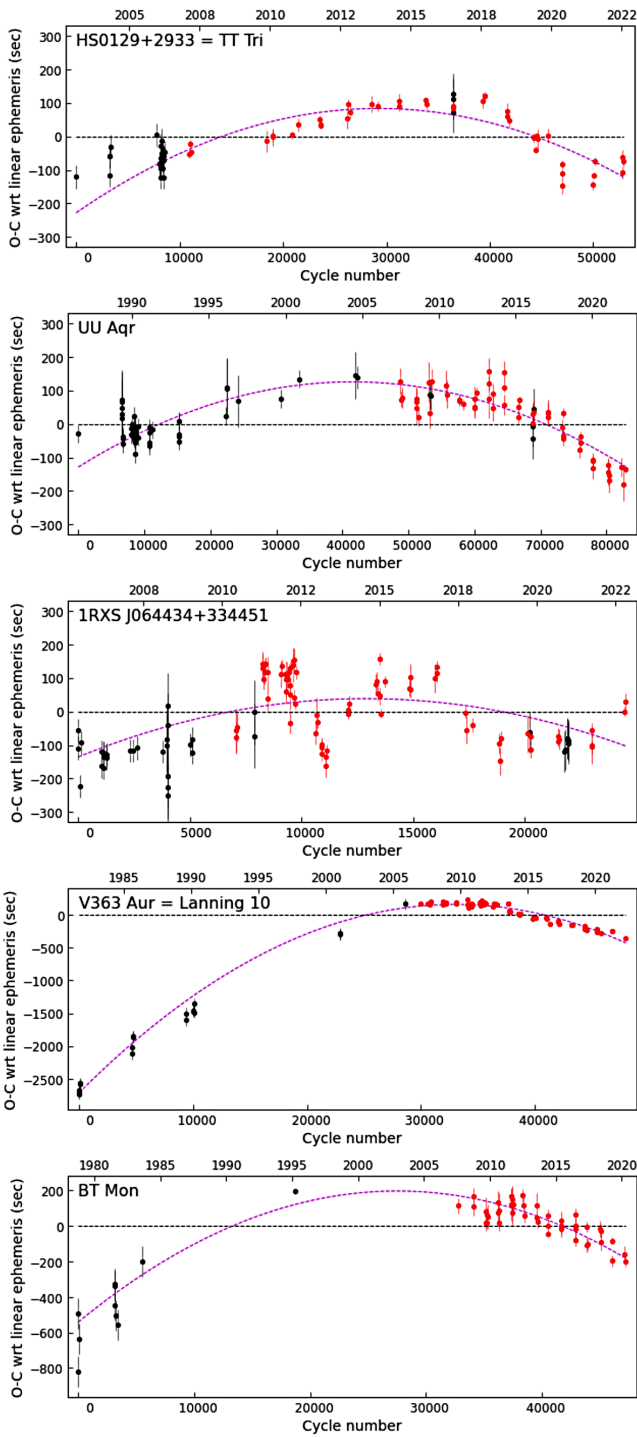


Figure 3. O–C diagrams with linear and quadratic ephemerides for stars showing stronger evidence of decreasing orbital periods. Color coding as in Figure 2.

Figure 4. O–C diagrams with linear and quadratic ephemerides for stars showing evidence of increasing orbital periods. Color coding as in Figure 2.

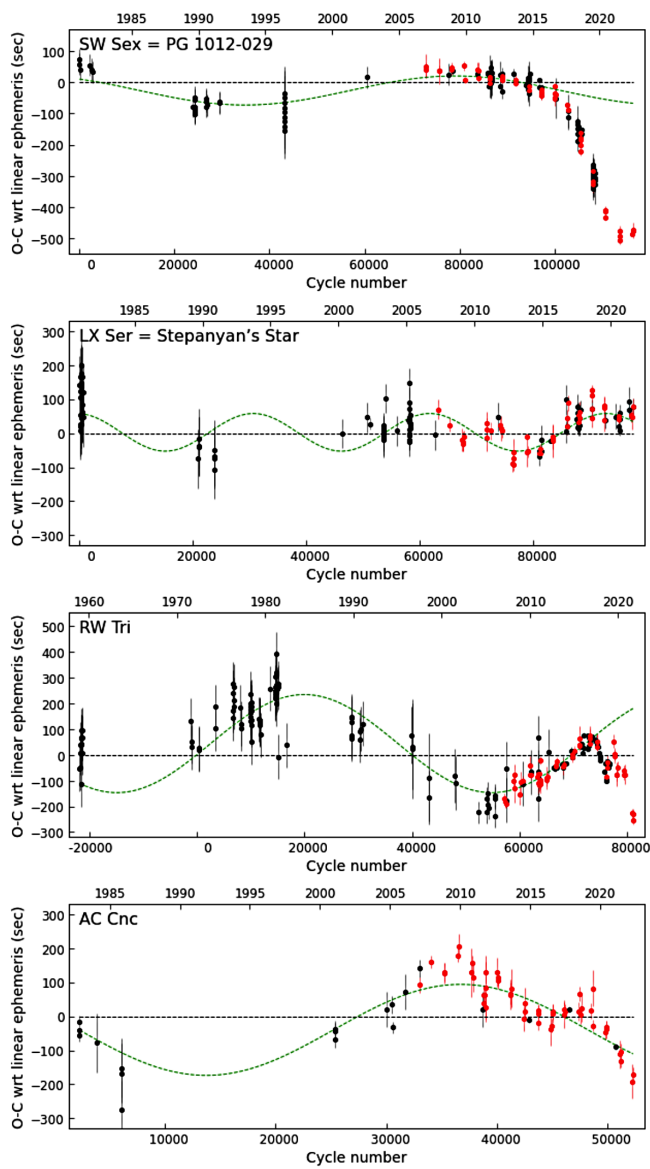


Figure 5. O–C diagrams with linear ephemerides and sinusoidal fits for stars showing evidence of sinusoidal variation in their orbital periods relative to a linear ephemeris. Color coding as in Figure 2 with sinusoidal fits dotted in green.

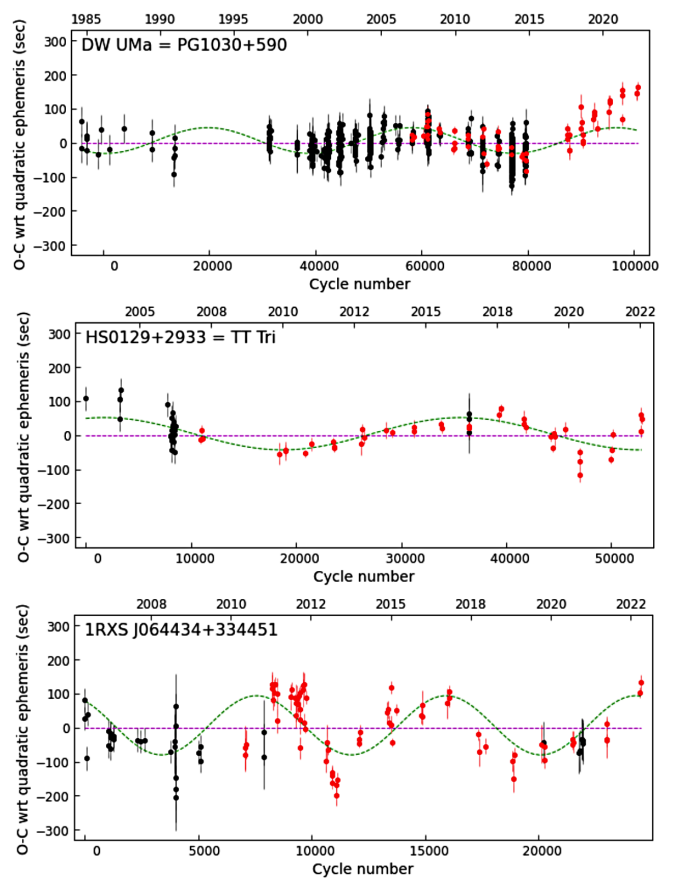


Figure 6. O–C diagrams with quadratic ephemerides and sinusoidal fits for stars showing evidence of sinusoidal variation in their orbital periods relative to a quadratic ephemeris. Color coding as in Figure 2 with sinusoidal fits dotted in green.

6. Interpretation

Several mechanisms have been proposed to explain relatively slow changes in the orbital periods of CVs above the period gap, including loss of angular momentum through magnetic braking associated with a magnetized stellar wind (Knigge *et al.* 2011), various versions of the Applegate mechanism associated with magnetically induced changes in the internal structure of the secondary star (Applegate 1992; Völschow *et al.* 2016; Lanza 2020), or a third body in the system whose presence causes a gravitationally induced oscillation of the eclipse time (Qian *et al.* 2013).

We do not believe there has been a sufficiently long period of observations to reach a firm conclusion on the long term behavior of any of the systems reported here. Whether the trends detected so far, as indicated by the fits applied to the O–C data, are maintained in the longer term only further observations will be able to determine. There have been numerous cases in the literature where attempts to assign a specific interpretation to apparently cyclical orbital behavior have failed to stand the test of time (Pulley *et al.* 2022). The dangers of interpreting observations as periodic when only two or three cycles may be present are outlined in Vaughan *et al.* (2016). We therefore do not attempt to assign physical significance to the fits shown in these O–C diagrams, but simply offer our measurements as data to anyone wishing to attempt such an interpretation in the future.

7. Summary

We report on a 17-year study to monitor the orbital periods of 18 eclipsing nova-like CVs referred to as SW Sex stars. We added 934 new eclipse times to 1338 times in the published literature and produced an O–C diagram for each star including all available data. This revealed clear trends in the behavior of most of the stars but also that many of the stars experienced deviations from these trends. We observed rapid and unusual decreases of 34 msec (a proportional change of -2.9×10^{-6}) in the orbital period of SW Sex during 2017 and of 46 msec (a proportional change of -2.3×10^{-6}) in the orbital period of RW Tri during 2018. DW UMa also appears to have recently diverged from the sinusoidal behavior it has been following for the past 30 years. It is clear from these results that observations will have to be maintained over a much longer timescale before definitive statements can be made about their long term behavior, or even whether stable long term behavior is likely for these stars. We intend to continue observing many of these stars.

8. Acknowledgements

I am grateful to the anonymous referee for a careful and helpful review. I am also grateful to Boris Gänsicke for his early encouragement to pursue this as a long-term project and to Chris Lloyd for helpful comments on an earlier draft. I acknowledge with thanks the observations of LX Ser by Cook and Dvorak in the AAVSO International Database and the use of AAVSO comparison charts and NASA’s Astrophysics Data System.

Software developed in the project made extensive use of the Astropy package (Astropy Collaboration 2018).

References

- Africano, J. L., and Klimke, A. 1981, *Inf. Bull. Var. Stars*, No. 1969, 1.
- Africano, J. L., Nather, R. E., Patterson, J., Robinson, E. L., and Warner, B. 1978, *Publ. Astron. Soc. Pacific*, **90**, 568.
- Andrae, R., Schulze-Hartung, T., and Melchior, P. 2010, “Dos and don’ts of reduced chi-squared” (<https://arxiv.org/pdf/1012.3754.pdf>).
- Applegate J. H., 1992, *Astrophys. J.*, **385**, 621.
- Ashoka, B. N., Seetha, S., Marar, T. M. K., Kasturirangan, K., Rao, U. R., and Bhattacharyya, J. C. 1994, *Astron. Astrophys.*, **283**, 455.
- Astropy Collaboration, *et al.* 2018, *Astron. J.*, **156**, 123.
- Baldwin, M. E., and Samolyk, G. 2005, *Observed Minima Timings of Eclipsing Binaries, No. 10*, AAVSO, Cambridge, MA.
- Baptista, R., Steiner, J. E., and Cieslinski, D. 1994, *Astrophys. J.*, **433**, 332.
- Bíró, I. B. 2000, *Astron. Astrophys.*, **364**, 573.
- Boyd, D. 2012, *J. Amer. Assoc. Var. Star Obs.*, **40**, 295.
- Boyd, D., *et al.* 2017, *Mon. Not. Roy. Astron. Soc.*, **466**, 3417.
- Bruch, A. 2022, *Mon. Not. Roy. Astron. Soc.*, **514**, 4718.
- Dhillon, V. S., Jones, D. H. P., and Marsh, T. R. 1994, *Mon. Not. Roy. Astron. Soc.*, **266**, 859.
- Dhillon, V. S., Jones, D. H. P., Marsh, T. R., and Smith, R. C. 1992, *Mon. Not. Roy. Astron. Soc.*, **258**, 225.
- Dhillon, V. S., Marsh, T. R., and Jones, D. H. P. 1991, *Mon. Not. Roy. Astron. Soc.*, **252**, 342.
- Dhillon, V. S., Marsh, T. R., and Jones, D. H. P. 1997, *Mon. Not. Roy. Astron. Soc.*, **291**, 694.
- Dhillon, V. S., Smith, D. A., and Marsh, T. R. 2013, *Mon. Not. Roy. Astron. Soc.*, **428**, 3559.
- Downes, R. A., Mateo, M., Szkody, P., Jenner, D. C., and Margon, B. 1986, *Astrophys. J.*, **301**, 240.
- Duerbeck, H. W. 1987, *ESO Messenger*, **50**, 8.
- Fang, X., and Qian, S. 2021, *Mon. Not. Roy. Astron. Soc.*, **501**, 3046.
- Fang, X., Qian, S., Han, Z., and Wang, Q. 2020, *Astrophys. J.*, **901**, 113.
- Garnavich, P. M., *et al.* 1990, *Astrophys. J.*, **365**, 696.
- Grauer, A. D., Ringwald, F. A., Wegner, G., Liebert, J., Schmidt, G. D., and Green, R. F. 1994, *Astron. J.*, **108**, 214.
- Green, E. M. 2008, private communication.
- Groot, P. J., Rutten, R. G. M., and van Paradijs, J. 2001, *Astron. Astrophys.*, **368**, 183.
- Hagen, H.-J., Groote, D., Engels, D., and Reimers, D. 1995, *Astron. Astrophys., Suppl. Ser.*, **111**, 195.
- Han, X. L., Zhang, L.-Y., Shi, J.-R., Pi, Q.-F., Lu, H.-P., Zhao, L.-B., Terheide, R. K., and Jiang, L.-Y. 2018, *Res. Astron. Astrophys.*, **18**, 68.
- Hellier, C. 1996, *Astrophys. J.*, **471**, 949.
- Hellier, C. 2001, *Cataclysmic Variable Stars*, Springer-Verlag, Berlin.
- Hellier, C., and Robinson, E. L. 1994, *Astrophys. J.*, **431**, L107.

- Henden, A. A., and Honeycutt, R. K. 1995, *Publ. Astron. Soc. Pacific*, **107**, 324.
- Henden, A. A., Templeton, M., Terrell, D., Smith, T. C., Levine, S., and Welch, D. 2018, VizieR Online Data Catalog: AAVSO Photometric All Sky Survey (APASS) DR10, II/336.
- Hernández Santisteban, J. V., Echevarría, J., Michel, R., and Costero, R. 2017, *Mon. Not. Roy. Astron. Soc.*, **464**, 104.
- Hoard, D. W., and Szkody, P. 1997, *Astrophys. J.*, **481**, 433.
- Hoard, D. W., Szkody, P., Froning, C. S., Long, K. S., and Knigge, C. 2003, *Astron. J.*, **126**, 2473.
- Honeycutt, R. K., Schlegel, E. M., and Kaitchuck, R. H. 1986, *Astrophys. J.*, **302**, 388.
- Horne, K. 1980, *Astrophys. J.*, **242**, L167.
- Horne, K., Lanning, H. H., and Gomer, R. H. 1982, *Astrophys. J.*, **252**, 681.
- Howell, S. B. 2006, *Handbook of CCD Astronomy*, 2nd ed., Cambridge Univ. Press, Cambridge.
- Kafka, S. 2021, Observations from the AAVSO International Database (<https://www.aavso.org/data-download>).
- Knigge, C., Baraffe, I., and Patterson, J. 2011, *Astrophys. J., Suppl. Ser.*, **194**, 28.
- Lanza, A. F. 2020, *Mon. Not. Roy. Astron. Soc.*, **491**, 1820.
- Li, K. *et al.* 2017, *Publ. Astron. Soc. Japan*, **69**, 28.
- Papadaki, C. *et al.* 2009, *J. Astron. Data*, **15**, 1.
- Patterson, J. 1984, *Astrophys. J., Suppl. Ser.*, **54**, 443.
- Penning, W. R., Ferguson, D. H., McGraw, J. T., Liebert, J., and Green, R. F. 1984, *Astrophys. J.*, **276**, 233.
- Pulley, D., Sharp, I. D., Mallett, J., and von Harrach, S. 2022, *Mon. Not. Roy. Astron. Soc.*, **514**, 5725.
- Qian, S.-B. *et al.* 2013, *Mon. Not. Roy. Astron. Soc.*, **436**, 1408.
- Qian, S.-B., Dai, Z.-B., He, J.-J., Yuan, J. Z., Xiang, F. Y., and Zejda, M. 2007, *Astron. Astrophys.*, **466**, 589.
- Robinson, E. L., Nather, R. E., and Kepler, S. O. 1982, *Astrophys. J.*, **254**, 646.
- Robinson, E. L., Shetrone, M. D., and Africano, J. L. 1991, *Astron. J.*, **102**, 1176.
- Rodríguez-Gil, P., Gänsicke, B. T., Barwig, H., Hagen, H.-J., and Engels, D. 2004, *Astron. Astrophys.*, **424**, 647.
- Rodríguez-Gil, P., *et al.* 2007, *Mon. Not. Roy. Astron. Soc.*, **377**, 1747.
- Rutten, R. G. M., van Paradijs, J., and Tinbergen, J. 1992, *Astron. Astrophys.*, **260**, 213.
- Sahman, D. I., Dhillon, V. S., Knigge, C., and Marsh, T. R. 2015, *Mon. Not. Roy. Astron. Soc.*, **451**, 2863.
- Schlegel, E. M., Honeycutt, R. K., and Kaitchuck, R. H. 1986, *Astrophys. J.*, **307**, 760.
- Schlegel, E. M., Kaitchuck, R. H., and Honeycutt, R. K. 1984, *Astrophys. J.*, **280**, 235.
- Schmidtobreick, L. 2015, in *Proceedings of The Golden Age of Cataclysmic Variables and Related Objects—III*, Palermo, Italy, <https://arxiv.org/pdf/1705.09332.pdf>.
- Seitter, W. C. 1984, *Astrophys. Space Sci.*, **99**, 95.
- Shafter, A. W., and Bautista, A., 2021, *Res. Notes AAS*, **5**, 207.
- Shafter, A. W., Hessman, F. V., and Zhang, E.-H. 1988, *Astrophys. J.*, **327**, 248.
- Shara, M. M., Mizusawa, T., Wehinger, P., Zurek, D., Martin, C. D., Neill, J. D., Forster, K., and Seibert, M. 2012, *Astrophys. J.*, **758**, 121.
- Sing, D. K., Green, E. M., Howell, S. B., Holberg, J. B., Lopez-Morales, M., Shaw, J. S., and Schmidt, G. D. 2007, *Astron. Astrophys.*, **474**, 951.
- Smak, J. 1995, *Acta Astron.*, **45**, 259.
- Smith, D. A., Dhillon, V. S., and Marsh, T. R. 1998, *Mon. Not. Roy. Astron. Soc.*, **296**, 465.
- Stanishev, V., Kraicheva, Z., Boffin, H. M. J., and Genkov, V. 2002, *Astron. Astrophys.*, **394**, 625.
- Stanishev, V., Kraicheva, Z., Boffin, H. M. J., Genkov, V., Papadaki, C., and Carpano, S. 2004, *Astron. Astrophys.*, **416**, 1057.
- Stanishev, V., Kraicheva, Z., and Genkov, V. 2006, *Astron. Astrophys.*, **455**, 223.
- Still, M. D. 1996, *Mon. Not. Roy. Astron. Soc.*, **282**, 943.
- Subebekova, G., Zharikov, S., Tovmassian, G., Neustroev, V., Wolf, M., Hernandez, M. -S., Kučáková, H., and Khokhlov, S. 2020, *Mon. Not. Roy. Astron. Soc.*, **497**, 1475.
- Thoroughgood, T. D., Dhillon, V. S., Watson, C. A., Buckley, D. A. H., Steeghs, D., and Stevenson, M. J. 2004, *Mon. Not. Roy. Astron. Soc.*, **353**, 1135.
- Thorstensen, J. R., Ringwald, F. A., Wade, R. A., Schmidt, G. D., and Norsworthy, J. E. 1991, *Astron. J.*, **102**, 272.
- Vaughan, S., Uttley, P., Markowitz, A. G., Huppenkothen, D., Middleton, M. J., Alston, W. N., Scargle, J. D., and Farr, W. M. 2016, *Mon. Not. Roy. Astron. Soc.*, **461**, 3145.
- Völschow, M., Schleicher, D. R. G., Perdelwitz, V., and Banerjee, R. 2016, *Astron. Astrophys.*, **587A**, 34.
- Walker, M. F. 1963, *Astrophys. J.*, **137**, 485.
- Warner, B. 1995, *Cataclysmic Variable Stars*, Cambridge Univ. Press, Cambridge.
- Warren, S. R., Shafter, A. W., and Reed, J. K. 2006, *Publ. Astron. Soc. Pacific*, **118**, 1373.
- Yamasaki, A., Okazaki, A., and Kitamura, M. 1983, *Publ. Astron. Soc. Japan*, **35**, 423.
- Young, P., Schneider, D. P., and Shectman, S. A. 1981, *Astrophys. J.*, **244**, 259.
- Zhang, E. 1987, *Acta Astrophys. Sinica*, **7**, 245.